Beyond Woods-Saxon and Perey-Buck paradigms from microscopic grounds

Guillaume Blanchon

CEA,DAM,DIF F-91297 Arpajon, France
Université Paris-Saclay, CEA, LMCE, 91680 Bruyères-le-Châtel, France

Hugo F. Arellano

Department of Physics - FCFM, U. Chile

ECT, Trento, June 16-21, 2024*

Content

Outline

Probes and targets

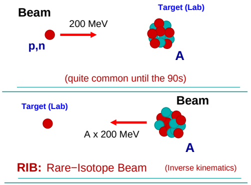

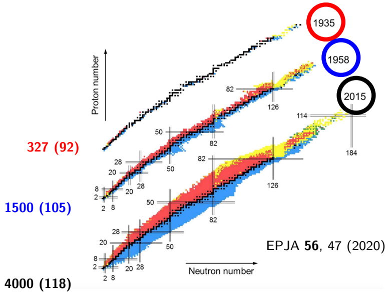

U_{NA} ?

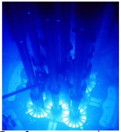

Nuclear reactors

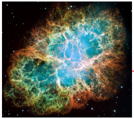

Supernovae

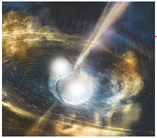

Neutron star mergers

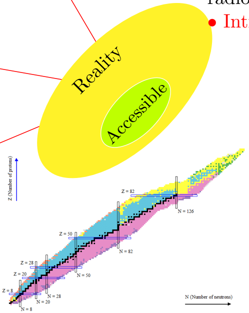

Nuclear landscape

Phenomenology: shapes & parameters

- Intuitive
- Simple and fast
- Global
- Suitable for evaluations and radioactive environments
- Intrinsic limitations by shapes

Theory

- Elaborate and cumbersome
- Challenging to calculate
- Limited success
- Can we unveil form factors?

▶ Microscopically driven optical potential

U_{NA}?

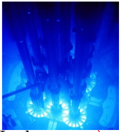

Nuclear reactors

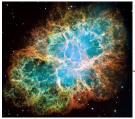

Supernovae

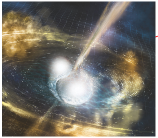

Neutron star mergers

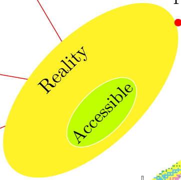

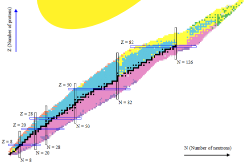

Nuclear landscape

Phenomenology: shapes & parameters

- Intuitive
- Simple and fast
- Global
- Suitable for evaluations and radioactive environments
- Intrinsic limitations by shapes

Theory

- Elaborate and cumbersome
- Challenging to calculate
- Limited success
- Can we unveil form factors?

▶ **Microscopically driven optical potential**

Potential is nonlocal, complex, energy dependent and dispersive

- **Antisymmetrization**

$$V_{HF}(\mathbf{r},\mathbf{r'}) = \int d\mathbf{r}_1 \rho(\mathbf{r}_1) v(\mathbf{r},\mathbf{r}_1) - \rho(\mathbf{r},\mathbf{r'}) v(\mathbf{r},\mathbf{r'})$$

- **Polarization**

  Surface term...

$$\Delta U(\mathbf{r},\mathbf{r}';E) = \sum_i V_{0i}(\mathbf{r}) G_{ii}(\mathbf{r},\mathbf{r'};E) V_{i0}(\mathbf{r'}),$$

  where G_{ii} is a propagator

$$V_{i0}(\mathbf{r}) = \beta_i r \frac{dU(r)}{dr} Y_\lambda^\mu(\widehat{\mathbf{r}}),$$

  transition potential in the Bohr collective model.

  A. Lev, W. P. Beres, and M. Divadeenam. PRC 9 :2416–2434, Jun 1974.

Potential is nonlocal, complex, energy dependent and dispersive

- **Antisymmetrization**

$$V_{HF}(\mathbf{r},\mathbf{r'}) = \int d\mathbf{r}_1 \rho(\mathbf{r}_1) v(\mathbf{r},\mathbf{r}_1) - \rho(\mathbf{r},\mathbf{r'}) v(\mathbf{r},\mathbf{r'})$$

- **Polarization**

  Surface term...

$$\Delta U(\mathbf{r},\mathbf{r}';E) = \sum_i V_{0i}(\mathbf{r}) G_{ii}(\mathbf{r},\mathbf{r'};E) V_{i0}(\mathbf{r'}),$$

where G_{ii} is a propagator

$$V_{i0}(\mathbf{r}) = \beta_i r \frac{dU(r)}{dr} Y_\lambda^\mu(\widehat{\mathbf{r}}),$$

transition potential in the Bohr collective model.

A. Lev, W. P. Beres, and M. Divadeenam. PRC 9 :2416–2434, Jun 1974.

Potential is nonlocal, complex, energy dependent and dispersive

- **Antisymmetrization**

$$V_{HF}(\mathbf{r},\mathbf{r'}) = \int d\mathbf{r}_1 \rho(\mathbf{r}_1) v(\mathbf{r},\mathbf{r}_1) - \rho(\mathbf{r},\mathbf{r'}) v(\mathbf{r},\mathbf{r'})$$

- **Polarization**
  Surface term...

$$\Delta U(\mathbf{r},\mathbf{r}';E) = \sum_i V_{0i}(\mathbf{r}) G_{ii}(\mathbf{r},\mathbf{r'};E) V_{i0}(\mathbf{r'}),$$

where G_{ii} is a propagator

$$V_{i0}(\mathbf{r}) = \beta_i r \frac{dU(r)}{dr} Y_\lambda^\mu(\widehat{\mathbf{r}}),$$

transition potential in the Bohr collective model.

A. Lev, W. P. Beres, and M. Divadeenam. PRC 9 :2416–2434, Jun 1974.

Woods and Saxon

$$V(r) = -[V_0 + iW_0] f_{vol}(r) - iW_D f_{surf}(r) - (U_{so} + iW_{so}) f_{surf}(r) \boldsymbol{\ell} \cdot \boldsymbol{\sigma}$$

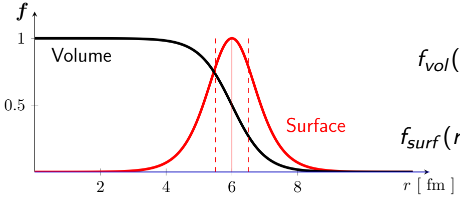

$$f_{vol}(r) \sim \frac{1}{1 + e^{(r-R_0)/a}}$$

$$f_{surf}(r) \sim \frac{4\, e^{(r-R_0)/a}}{[1 + e^{(r-R_0)/a}]^2}$$

Integro-différential scattering equation

$$-\frac{\hbar^2}{2\mu}\Delta\psi(\mathbf{r})+\int V_{NL}(\mathbf{r},\mathbf{r'})\psi(\mathbf{r'})\mathrm{d}\mathbf{r'}=E\psi(\mathbf{r}),$$

When potential is local

$$V_{NL}(\mathbf{r},\mathbf{r'})=V_L(\mathbf{r})\delta(\mathbf{r},\mathbf{r'}).$$

Scattering equation reduces to **differential**,

$$-\frac{\hbar^2}{2\mu}\Delta\psi(\mathbf{r})+V_L(\mathbf{r})\psi(\mathbf{r})=E\psi(\mathbf{r}).$$

$\rightarrow$ **Need for numerical tools**

SIDES: Schrödinger Integro-Differential Equation Solver

G. Blanchon, M. Dupuis, H. F. Arellano, R. N. Bernard, B. Morillon, CPC 254 (2020) 107340

- Method: modified Numerov method
- Extension for potentials with first derivative

  (G. Blanchon, M. Dupuis, H. F. Arellano, R. N. Bernard, B. Morillon, P. Romain, EPJA (2021) 57:13)
- Available with pairing *(not published yet)*

SWANLOP: Scattering WAves off NonLocal Optical Potentials

H. F. Arellano, G. Blanchon, CPC 259 (2021) 107543

- Lippmann-Schwinger equation
- Momentum and coordinate space potentials

H. F. Arellano, G. Blanchon, PLB 789 (2019) 256-261

$V(r, r', E) \rightarrow \frac{d\sigma}{d\Omega}$, $\sigma_{E,R,T}$, A_y, **phaseshifts, wave functions**

Potentials included in SWANLOP & SIDES

- Koning-Delaroche global local potential *(n/p below 200 MeV)*

  A. J. Koning and J.-P. Delaroche NPA 713(3-4) 231 - 310, 2003.

- Morillon-Romain global dispersive local potential *(n/p below 200 MeV)*

  B. Morillon and P. Romain. PRC, 70 014601 (2004) and PRC, 76(4) 044601 (2007).

- Perey-Buck global nonlocal potential *(n below 30 MeV)*

  F. Perey and B. Buck. Nucl. Phys., 32 353 – 380, 1962.

- Tian-Pang-Ma global nonlocal potential *(below 30 MeV)*

  Y. Tian, D.-Y. Pang, and Z.-Y. Ma. IJMP E, 24(01) 1550006, 2015.

- Potentials given on a radial mesh

Potential in forthcoming versions

- Morillon global dispersive nonlocal potential *(n below 200 MeV)*

  B. Morillon, G. Blanchon, P. Romain and H. F. Arellano PRC, 109, 044611 (2024)

Outline

2.E

Nuclear Physics **32** (1962) 353—380; © *North-Holland Publishing Co., Amsterdam*

A NON-LOCAL POTENTIAL MODEL FOR THE SCATTERING OF NEUTRONS BY NUCLEI

F. PEREY and B. BUCK

Oak Ridge National Laboratory † *Oak Ridge, Tennessee*

Received 25 September 1961

Abstract: An energy independent non-local optical potential for the elastic scattering of neutrons from nuclei is proposed and the wave-equation solved numerically in its full integro-differential form. The non-local kernel is assumed separable into a potential form factor times a Gaussian non-locality. The potential form factor, of argument $\frac{1}{2}(\mathbf{r}+\mathbf{r}')$, is that of a real Saxon form plus an imaginary term having the shape of the derivative of a Saxon form. A real local spin-orbit potential of the usual Thomas form is included. The parameters of the potential obtained solely from the fitting of the differential cross sections for lead at 7 MeV and 14.5 MeV are used unchanged to calculate the elastic differential cross sections, total and reaction cross sections and polarizations on some elements ranging from Al to Pb at various energies from 0.4 MeV to 24 MeV. The S-wave strength functions and the effective scattering radius R' are also calculated with the same parameters. The parameters in the usual notations are: real potential $V = 71$ MeV, $r = 1.22$ fm, $a = 0.65$ fm; surface imaginary potential $W = 15$ MeV, $a = 0.47$ fm; non-locality $\beta = 0.85$ fm; spin-orbit potential, using the nucleon mass in the Thomas form, $U_{so} = 1300$ MeV. The energy independence of the

F. PEREY AND B. BUCK

linate representation, a non-local potential operating on a w
; the form

$$V\Psi(\mathbf{r}) = \int V(\mathbf{r}, \mathbf{r}')\Psi(\mathbf{r}')\mathrm{d}\mathbf{r}'.$$

faced with an integro-differential Schrödinger equation whic
y by numerical integration and iteration.
al grounds it is necessary that the kernel function $V(\mathbf{r},$
, i.e.,

$$V(\mathbf{r}, \mathbf{r}') = V(\mathbf{r}', \mathbf{r}).$$

te the numerical calculations a separable form was chosen fo
rnel function:

$$V(\mathbf{r}, \mathbf{r}') = U\left(\frac{\mathbf{r}+\mathbf{r}'}{2}\right) H\left(\frac{\mathbf{r}-\mathbf{r}'}{\beta}\right).$$

nonlocality

Gaussian nonlocality

$$H_\beta(|\mathbf{r}'-\mathbf{r}|) = \frac{e^{-|\mathbf{r}'-\mathbf{r}|^2/\beta^2}}{\pi^{3/2}\beta^3}$$

$$H_\beta(|\mathbf{r}'-\mathbf{r}|) \underset{\beta\to 0}{=} \delta(\mathbf{r}'-\mathbf{r})$$

$\beta \approx 0.85$ fm

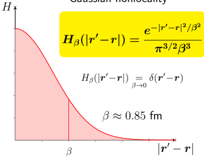

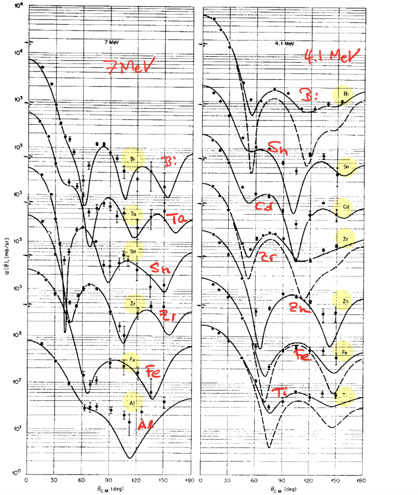

Fig. 2. Comparison of predictions of the energy independent non-local optical model with experimental elastic differential cross-sections of neutrons at 4.1 MeV and 7 MeV. The parameters are

Perey-Buck's assumptions:

- Separability
- Gaussian nonlocality
- Low incident energy $E < 24$ MeV
- Energy-independent
- Local spin-orbit

$\rightarrow$ Shape used in most of nowadays phenomenology

$\rightarrow$ Is it validated by microscopy? (at least by a given microscopic model)

Perey-Buck's assumptions:

- Separability
- Gaussian nonlocality
- Low incident energy $E < 24$ MeV
- Energy-independent
- Local spin-orbit

$\rightarrow$ Shape used in most of nowadays phenomenology

$\rightarrow$ Is it validated by microscopy? (at least by a given microscopic model)

Perey-Buck's assumptions:

- Separability
- Gaussian nonlocality
- Low incident energy $E < 24$ MeV
- Energy-independent
- Local spin-orbit

$\rightarrow$ Shape used in most of nowadays phenomenology

$\rightarrow$ Is it validated by microscopy? (at least by a given microscopic model)

Outline

Microscopic optical model

NN scattering data + deuteron properties

$$\delta_L(E) \to \begin{cases} E_{cm} \lesssim m_\pi c^2 \sim 140 \text{ MeV} \\ E_{cm} \gtrsim m_\pi c^2 \quad \text{non-Hermitian} \end{cases}$$

v_{NN} + NNN + …

finite nuclei: $A+1$

structure: $E<0$

- Ground state
- s.p. excitations
- collective excitations

D1,D1S,DG,...
M3Y
Skyrme

scattering: $E>0$

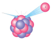

- Elastic •
- Quasi-elastic
- Inelastic

Watson multi-scattering
Kerman-McManus-Thaler
Folding model
JLM local dens. approx.

$\infty+1$: infinite nuclear matter

SCGF
BBG
BHF •

Effective interaction $g[\rho;E]$: •
Nonlocal, ρ- and E-dependent
Mass operator: $\Sigma[\rho;E]$ (JLM)

Equation of State
g_{NN} as it comes •
g_{NN} localized (approx.)

Melbourne •
von Geramb
Brieva-Rook

$g_{NN} = g_C + \boldsymbol{L}\cdot\boldsymbol{S}\, g_{LS} + \hat{S}_{12}\, g_T$ •

Effective interaction

- v_{eff} is, in general, *non local*: $\langle r_2|v|r_1\rangle = v(r_2, r_1) \rightarrow f(r_1)\delta(r_2 - r_1)$
- v_{eff} is complex... $\rightarrow$ absorption.
- v_{eff} is obtained from the *bare* nucleon-nucleon interaction
- v_{eff} depends on the energy and density. In general, v_{eff} is target dependent.
- At high energies $v \sim t$, the scattering matrix.
- v_{eff} can be represented as:
  - Local functions
  - Sums of 'Yukawas': $\sim \sum_k g_k \, e^{-\mu_k r}/r$
  - Zero-range (Skyrme) interactions: $\sim g_k \delta(\vec{r})$

Microscopic optical model

Bare $NN \to N + A$ connection

$$\underbrace{\boldsymbol{NN} \to \left\{ \begin{array}{c} \left(\frac{d\sigma}{d\Omega}\right)_{NN} \\ \downarrow\uparrow \\ \delta_L(E) \end{array} \right\}}_{\text{2-Body}} \rightleftharpoons v_{NN} \underbrace{\begin{array}{c} \nearrow \quad \mathscr{G}_{NN} \\ \searrow \quad t_{NN} \end{array} \Bigg\}}_{\text{Effective interaction}} \underbrace{\to \underbrace{U_{opt}(\mathbf{k}', \mathbf{k}; E)}_{\uparrow\, |\Psi_{g.s.}\rangle} \to \left\{ \begin{array}{c} |\psi\rangle \\ \frac{d\sigma}{d\Omega} \\ \sigma \end{array} \right.}_{\text{N+A}}$$

$$U(\mathbf{k}', \mathbf{k}; E) = \int d\mathbf{p} d\mathbf{p}' \quad \underbrace{\rho(\mathbf{p}', \mathbf{p})}_{\sim \sum \phi_\alpha(p')\phi_\alpha^\dagger(p)} \quad \underbrace{\langle \mathbf{k}'\, \mathbf{p}' \,|G(E,\rho)|\, \mathbf{k}\, \mathbf{p} \rangle}_{V_{NN}}$$

- In-medium folding potentials based on density-dependent BHF *g* matrix.
- Bare *NN* potentials: N3LO *(Entem and Machleidt PRC (2003))* and Argonne v_{18} *(Wiringa, Stoks and Schiavilla PRC (1995))*.
- Folding potentials evaluated in momentum space.
- Scattering observables obtained from `SIDES` and `SWaNLOP` packages [Comput. Phys. Commun. 254, 107340 (2020); Comput. Phys. Commun. 259, 107543 (2021).]
- Perey-Buck parametrizations from Tian et al [Int. J. Mod. Phys. E 24(01), 1550006 (2015)].
- Reasonable results over 10-300 MeV energy span.

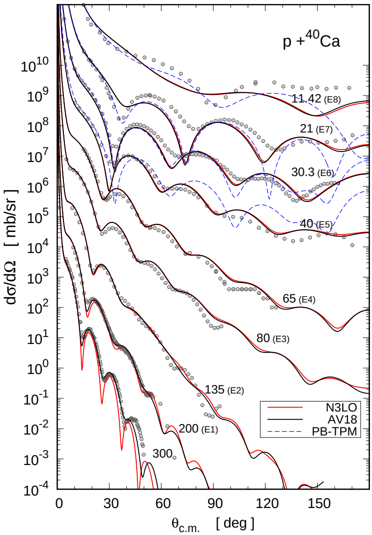

s-wave potential for p+^{40}Ca scattering at 65 MeV

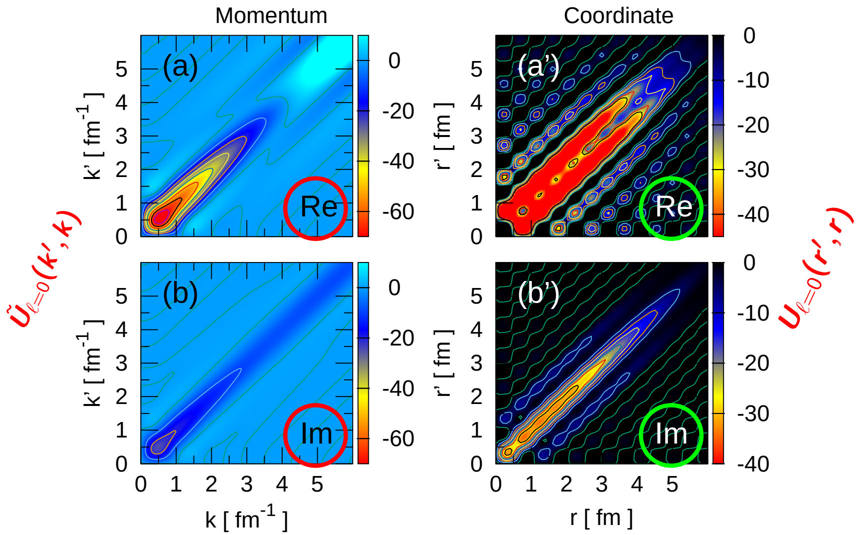

EPJA **57, 27 (2022)**

Representations
$\langle \text{post} | \hat{U} | \text{prior} \rangle$

relative coordinates

$r', r, \hat{\boldsymbol{r}} \cdot \hat{\boldsymbol{r}}'$

$\mathscr{U}(\boldsymbol{r}', \boldsymbol{r})$

Fourier →

← Fourier

relative momenta

$k', k, \hat{\boldsymbol{k}} \cdot \hat{\boldsymbol{k}}'$

$\tilde{\mathscr{U}}(\boldsymbol{k}', \boldsymbol{k})$

$\updownarrow$ $\updownarrow$

'nonlocality'

$$\boldsymbol{R} = \frac{1}{2}(\boldsymbol{r}' + \boldsymbol{r})$$
$$\boldsymbol{s} = \boldsymbol{r}' - \boldsymbol{r}$$

$$\boldsymbol{q} = \boldsymbol{k}' - \boldsymbol{k}$$
$$\boldsymbol{K} = \frac{1}{2}(\boldsymbol{k}' + \boldsymbol{k})$$

momentum transfer

'current'

$s, R, \hat{\boldsymbol{R}} \cdot \hat{\boldsymbol{s}}$

$K, q, \hat{\boldsymbol{K}} \cdot \hat{\boldsymbol{q}}$

$$\tilde{\mathscr{U}}(\boldsymbol{k}', \boldsymbol{k}) \rightleftarrows \tilde{U}(\boldsymbol{K}, \boldsymbol{q}) = \tilde{U}(K, q; w)$$

$\tilde{U}(K,q)$ in the Kq plane

Weak angular dependence ($w = \hat{K}\cdot\hat{q}$) $\rightarrow$ n=0

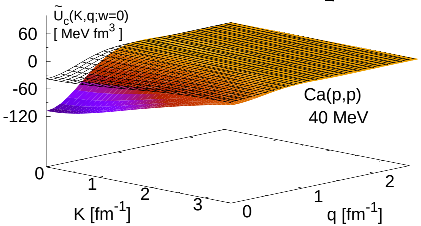

$$\tilde{\mathscr{U}}(\boldsymbol{k}',\boldsymbol{k}) = \sum_{l=0}^{\infty}(2l+1)\tilde{U}_l(k,k')P_l(\hat{k}\cdot\hat{k}')$$

$$\tilde{U}(\boldsymbol{K},\boldsymbol{q}) = \sum_{n=0}^{\infty}(2n+1)\tilde{U}_n(K,q)P_n(\hat{K}\cdot\hat{q})$$

$$\tilde{U}(K,q) = \frac{\tilde{U}(K,q)}{\tilde{U}(K,0)} \times \frac{\tilde{U}(K,0)}{\tilde{U}(0,0)} \times \tilde{U}(0,0) \equiv \tilde{V}(K,q) \times \tilde{H}(K) \times W$$

Nonlocality

Strength

Weak K-dependence !

$\tilde{V}_c(K,q) = \tilde{U}(K,q)/\tilde{U}(K,0) \sim \tilde{v}(q)$ in the range 10–300 MeV

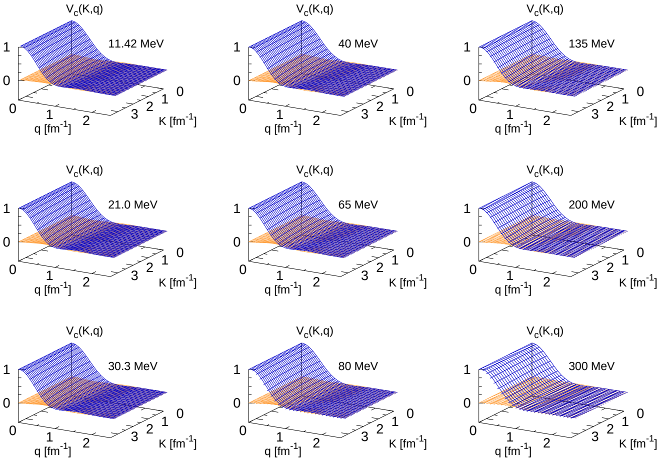

Real
Imaginary

K-independent

$$K = 0 \to V_c(K,q) \sim \tilde{v}(q)$$

Nonlocality *vs.* Perey-Buck

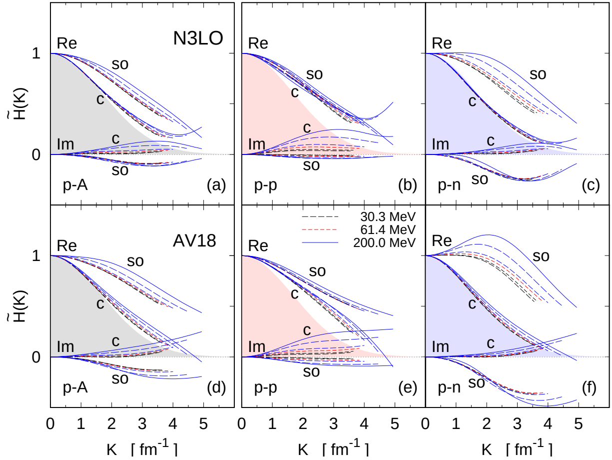

$$H_{PB}(s) = \frac{1}{\pi^{3/2}\beta^3} e^{-s^2/\beta^2}$$

$$\tilde{H}_{PB}(K) = e^{-\beta^2 K^2/4}$$

Nonlocalities for n+A & p+A

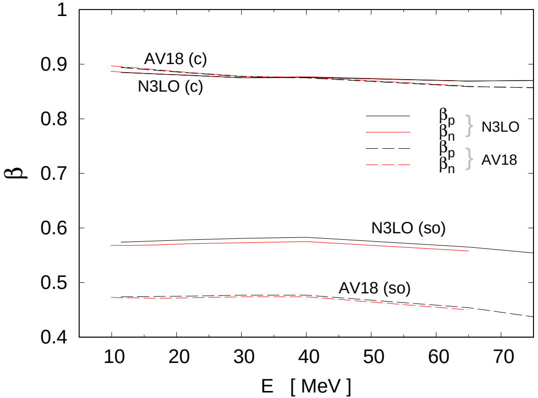

Nonlocalities for n+A & p+A

		N3LO			AV18		
	Energy (MeV)	β_{pA} (fm)	β_{pp} (fm)	β_{pn} (fm)	β_{pA} (fm)	β_{pp} (fm)	β_{pn} (fm)
Central	11.42	0.89	0.72	0.94	0.89	0.73	0.95
	21.0	0.88	0.72	0.94	0.89	0.72	0.94
	30.3	0.88	0.71	0.93	0.88	0.71	0.94
	40.0	0.88	0.71	0.93	0.88	0.71	0.93
	61.4	0.87	0.72	0.93	0.86	0.70	0.92
	80.0	0.87	0.72	0.93	0.86	0.71	0.92
	135.0	0.87	0.75	0.92	0.83	0.71	0.89
	200.0	0.86	0.78	0.90	0.80	0.72	0.85
Spin-orbit	11.42	0.57	0.61	0.51	0.47	0.58	0.03
	21.0	0.58	0.61	0.50	0.46	0.59	—
	30.3	0.58	0.62	0.49	0.48	0.59	—
	40.0	0.58	0.63	0.48	0.48	0.60	—
	61.4	0.57	0.63	0.43	0.46	0.60	—
	80.0	0.55	0.62	0.37	0.37	0.59	—
	135.0	0.48	0.59	0.13	0.32	0.56	—
	200.0	0.44	0.56	—	0.22	0.51	—

$\tilde{U}(0,0)$ & Volume integral

In coordinate space, the nonlocal optical potential $U(\vec{r},\vec{r'})$ is related to the momentum-space potential $U(\vec{k},\vec{k'})$ through a Fourier transform:

$$U(\vec{r},\vec{r'}) = \iint U(\vec{k},\vec{k'}) e^{i(\vec{k}\cdot\vec{r}-\vec{k'}\cdot\vec{r'})}\, d^3k\, d^3k'$$

Volume Integral in Momentum Space

The volume integral of the potential in momentum space is:

$$J(U) = \iint U(\vec{k},\vec{k'})\, d^3k\, d^3k'$$

Connection to $U(0,0)$

$$U(\vec{k},\vec{k'}) = \frac{1}{(2\pi)^3} \iint U(\vec{r},\vec{r'}) e^{-i(\vec{k}\cdot\vec{r}-\vec{k'}\cdot\vec{r'})}\, d^3r\, d^3r'$$

At the origin $\vec{k} = \vec{0}$ and $\vec{k'} = \vec{0}$:

$$U(0,0) = \frac{1}{(2\pi)^3} \iint U(\vec{r},\vec{r'})\, d^3r\, d^3r'$$

Therefore, $U(0,0)$ is proportional to the volume integral of the potential in coordinate space:

$$U(0,0) = \frac{J(U)}{(2\pi)^3}$$

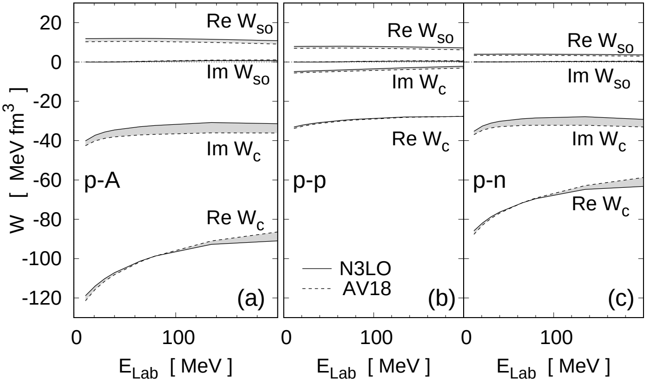

Volume integral

$$W = \frac{J}{(2\pi)^3}$$

JvH factorization

$$U(K,q) \approx \frac{J}{(2\pi)^3}\; v(q)\; H(K)$$

(H. F. Arellano, G. Blanchon EPJA (2022) 58 :119)

Microscopic potential *vs.* JvH

p+^{40}Ca

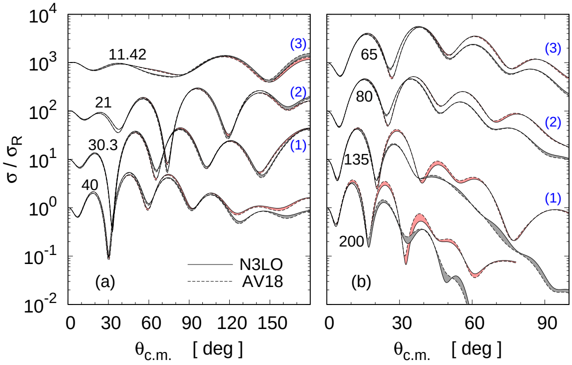

Discrepancies above 30 MeV

p + ^{40}Ca @ 200 MeV & *n*-expansion

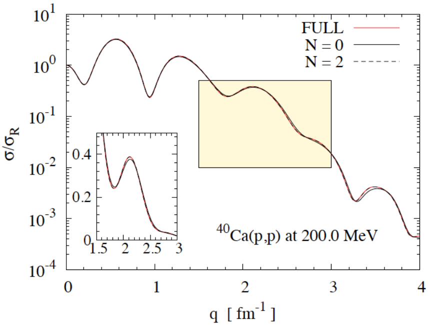

Figure 1: Ratio-to-Rutherford differential cross section as a function of the momentum transfer for p + ^{40}Ca at 200 MeV. Red curves correspond to the full potential, whereas solid and dashed black curves represent results in Kq–repesentation truncated at $N = 0$ and 2, respectively. The inset shows a close-up in linear scale.

Potential is separable

(G. Blanchon, H. F. Arellano, EPJ Web of Conferences 292, (2024))

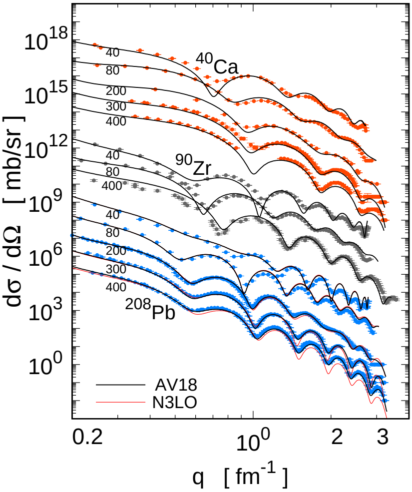

Figure 1: Differential cross section for proton-nucleus elastic scattering as function of the momentum transfer based on AV18 (black curves) and N3LO (red curves) bare potentials.

JvH factorization (second try)

$$U(K,q) \approx \frac{J}{(2\pi)^3}\ v(k_0,q)\ H(K)$$

with k_0 the on-shell momentum in the c.m. reference frame.

(H. F. Arellano, G. Blanchon PRC 109, 064609 (2024))

Nonlocality form factor - 200 MeV

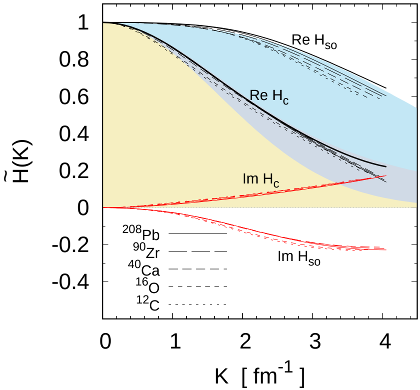

$$\tilde{H}(K) = \frac{1}{[1+\eta(K)]^2} \frac{1+i\alpha(K)}{1-i\alpha(K)}$$

If $\alpha = 0$ and $\eta \sim b^2K^2$, then

$$H(s) \sim \frac{e^{-s/b}}{8\pi b^3} \qquad \text{(hydrogenic)}$$

vs

$$H(s) \sim \frac{e^{-s^2/b^2}}{\pi^{3/2} b^3} \qquad \text{(Gaussian)}$$

Unveiling radial shapes (I)

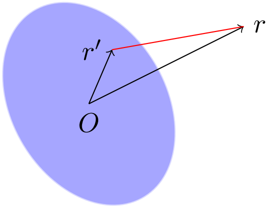

$$\tilde{V}(\boldsymbol{q}) = \tilde{\rho}(\boldsymbol{q})\tilde{v}(\boldsymbol{q})$$

$$V(\boldsymbol{r}) = \iiint \rho(\boldsymbol{r}')d^3r'v(\boldsymbol{r}-\boldsymbol{r}')$$

Unveiling radial shapes (II)

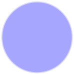

$$\tilde{\rho}(q) = 3\frac{j_1(qR)}{qR} \equiv \rho_{SL}(q)$$

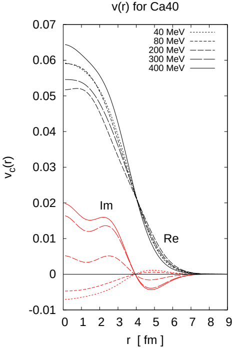

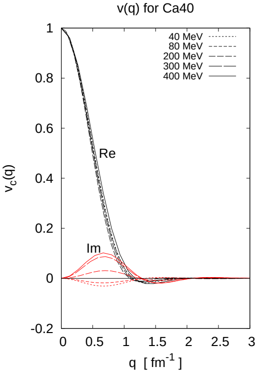

$$\rho_{SL}(q)\ \frac{1}{1+b^2q^2}$$

hard sphere⊗Yukawa

$$\rho_{SL}(q)\ e^{-a^2q^2}$$

hard sphere⊗Gaussian

$$\rho_{SL}(q)\ \frac{1}{(1+b^2q^2)^2}$$

hard sphere⊗hydrogenic

$$\rho_{SL}(q)\ e^{-a^2q^2}\ \frac{1}{1+b^2q^2}$$

soft sphere⊗Yukawa

Imaginary contribution ↔ second derivative of the real part

$$\mathrm{Re}\left[\tilde{v}_{c,so}(q)\right] = \tilde{\rho}_{SL}(qR_x)\, e^{-a_x^2 q^2}\, \frac{1}{1+b_x^2 q^2}, \tag{1a}$$

$$\mathrm{Im}\left[\tilde{v}_{c,so}(q)\right] = c_y\, q^2 \tilde{\rho}_{SL}(qR_y)\, e^{-a_y^2 q^2}\, \frac{1}{1+b_y^2 q^2}. \tag{1b}$$

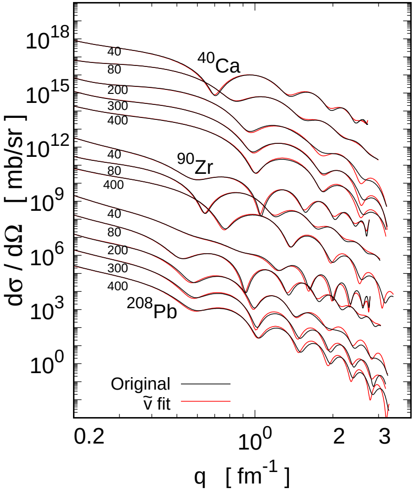

Figure 2: Differential cross sections as functions of the momentum transfer based on the microscopic folding model (black curves) and global fit for $\tilde{v}(q)$ (red curves).

Outline

Concluding remarks

1. Unveiled the nonlocal structure of the optical potential, providing quantitative account for phenomenological bell-shape Perey-Buck nonlocality.
2. Findings based on microscopic approach for NA scattering, folding density-dependent g matrices from realistic NN potentials.
3. The spin-orbit coupling is also nonlocal. We find $\beta_{so} \sim 0.45 - 0.58$ fm^{-1}.
4. Approach allows for selective exploration of scalar/isoscalar components of the potential.
5. JvH factorization constitutes an interesting framework for refined phenomenological parametrizations.

What about going higher in energy?

Building the potential

$$\tilde{\mathcal{U}}(\boldsymbol{k}', \boldsymbol{k}; E) = \tilde{\mathcal{U}}_c(\boldsymbol{k}', \boldsymbol{k}; E) + i\boldsymbol{\sigma}\cdot\hat{\boldsymbol{n}}\,\tilde{\mathcal{U}}_{so}(\boldsymbol{k}', \boldsymbol{k}; E)$$

$$\tilde{\mathcal{U}}_\nu(\boldsymbol{k}', \boldsymbol{k}; E) = 4\pi \sum_{\alpha=p,n} \int_0^\infty z^2 dz\, \rho_\alpha(z)\, j_0(qz) \int d\boldsymbol{P}\, S_z(P) \left\langle \frac{\boldsymbol{k}'-\boldsymbol{P}}{2} \right| g^{\nu\alpha}_{\bar{K}}(\rho_z, E+\bar{\epsilon}) \left| \frac{\boldsymbol{k}-\boldsymbol{P}}{2} \right\rangle_{\mathcal{A}}$$

$$S_z(P) = \frac{3}{4\pi k_z^3}\,\Theta(k_z - P)$$

$$k_z = \left[\frac{3\pi^2 \rho(z)}{2}\right]^{1/3}$$

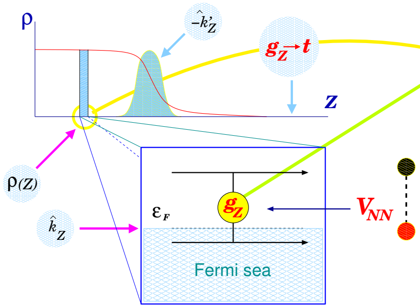

$U_{pA} = U_{pN} + U_{pP}$
$U_{nA} = U_{nN} + U_{nP}$